

# Determination of cavities using electrical resistivity tomography

René PUTIŠKA<sup>1</sup>, Maroš NIKOLAJ<sup>2</sup>, Ivan DOSTÁL<sup>1</sup>, David KUŠNIRÁK<sup>1</sup>

<sup>1</sup> Department of Applied and Environmental Geophysics, Faculty of Natural Sciences  
Comenius University, Mlynská dolina, pav. G, 842 48 Bratislava, Slovak Republic  
e-mail: putiska@fns.uniba.sk; dostal@fns.uniba.sk; kushnirak@fns.uniba.sk

<sup>2</sup> Water Constructions Building Company (state enterprise)  
Karloveská 2, 84105 Bratislava, Slovak Republic; e-mail: maros.nikolaj@vzb.sk

**Abstract:** Geophysical surveys for cavity detection are one of the most common near-surface applications. The usage of resistivity methods is also very straightforward for the air-filled underground voids, which should have theoretically infinite resistivity in the ERT image. In the first part of the paper, we deal with the comparison of detectability of the cavity by several types of the electrode arrays, the second part discusses the effect of a thin layer around the cavity itself, by means of 2D modelling. The presence of this layer deforms the resistivity image significantly as the resistive anomaly could be turned into a conductive one, in the case when the thin layer is more conductive than the background environment. From the electrical array analysis for the model situation a dipole-dipole and combined pole-dipole shows the best results among the other involved electrical arrays.

**Key words:** electrical resistivity tomography, cavity, resistivity modelling, resistivity inversion

## 1. Introduction

Geophysical methods can provide useful subsurface information and they are in common use for detection of different underground voids such as corridors, crypts, cellars, caves and others. These voids can be empty, full or partly water-filled or filled with different kind of stuff. Different prospecting techniques have been employed to detect underground voids. Success depends on their ability to reach the target depth with the appropriate resolution for each problem.

Electrical resistivity techniques were used in cave detection (*Cook and Nostrand, 1954; Vincenz, 1968; Dutta et al., 1970; Greenfield, 1979; Militzer et al., 1979; Smith, 1986*). *Thomas and Roth (1999)* presented a comparison study between 12 methods (including four geophysical techniques) for sinkhole and void detection. *Hutchinson et al. (2002)* provided a useful comparison of various geophysical approaches for void detection. Contribution of geophysical methods to karst-system exploration was completed by *Chalikakis et al. (2011)*. *Cardarelli et al. (2006a)* use electrical resistivity tomography to detect buried cavities in Rome.

Geophysical methods aim to characterise the variations of the physical parameters of underground formations. Geophysical measurements produce a set of data in which various parameters are measured. Each of these parameters is related to one or more physical properties of the subsurface and to their spatial distribution (*Chalikakis et al., 2011*). For this type of problem, electrical resistivity tomography (ERT), is a popular choice due to the low costs of the survey and the high resistivity contrast that exists between the air-filled cavity and the surrounding formation (*Van Schoor, 2002; Zhou et al., 2002*). The cavities can be also partially or completely water-filled and, depending on the composition of the water, can have a resulting electrical conductivity ranging from very conductive to relatively resistive, compared to the host rock (*Chalikakis et al., 2011*).

But here is another situation, a thin conductivity layer around air-filled cavities. It is natural that around the wall of different underground voids is the thin layer of water with clay mineral due to soil moisture and soil water. Usually this thin layer has much higher conductivity than surrounding areas. Has this layer real effect to the result of electrical resistivity tomography? A frequently occurring problem with ERT is the need to determine which of the many existing electrode configurations will respond best to the material changes. Each array has distinctive advantages and disadvantages in terms of depth of investigation, sensitivity to horizontal or vertical variations, and signal strength (*Loke, 1997; Zhou et al., 2002*). Comparison of the responses of dipole-dipole (DD), Wenner alpha (WA), Schlumberger (SCH), combined pole-dipole (CPD) electrode arrays have been computed using the 2D finite difference method and discussed in this paper.

## 2. The synthetic test

In that case, the cavity is filled with air, ERT indicates high resistivity (Fig. 1), but what is an ERT result when the thin very conductive layer is around the cavity? This section introduces a synthetic example that variability of resistivity values depends on resistivity or conductivity changes in very thin layer. The intention is to illustrate the results that can be obtained by ERT inversion. The resistivity synthetic model is displayed in Fig. 1 and contains one highly resistive circle anomaly  $\rho_3$  of  $1e6 \Omega m$ , representing theoretically infinite resistivity. The background resistivity  $\rho_1$  is set to  $100 \Omega m$ . During the test two different resistivity parameters  $\rho_2$  have been used for the thin layer ( $0.1 \Omega m$  and  $100 \Omega m$ ) so the ratio  $\rho_2/\rho_1$  is 0.001 and 1.0 respectively, what mean that the thin layer around the cavity has the same parameters as the surrounding environment in the first case (Fig. 2) and in the second case the layer is highly conductive (Fig. 3).

A synthetic data set was computed for all involved electrode arrays (DD, WA, SCH and CPD) with 48 electrodes at 0.5 m spacing, what leads to a 23.5 m long profile. Both the smoothness constrained inversion  $\mathbf{I}_2$  (Cardarelli and Fischanger, 2006b) and the  $\mathbf{I}_1$  norm inversion (Olayinka and Yaramanci, 2000; Loke et al., 2003) were tested on this synthetic data set. The  $\mathbf{I}_2$  norm inversion method gives optimal results where the subsurface geology exhibits a smooth variation, such as the diffusion boundary of a chemical plume. However, in cases where the subsurface consists of bodies that are internally homogeneous with sharp boundaries (such as a cave), this method tends to smear out the boundaries. The  $\mathbf{I}_1$  norm or blocky optimi-

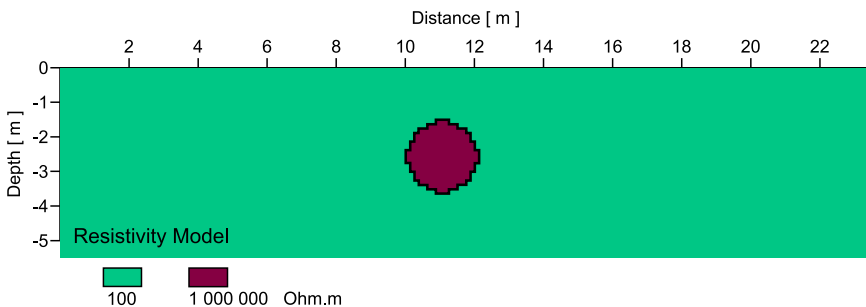


Fig. 1. Resistivity model, length of profile is 23.5 m, centre of anomaly is  $x = 11$  m.

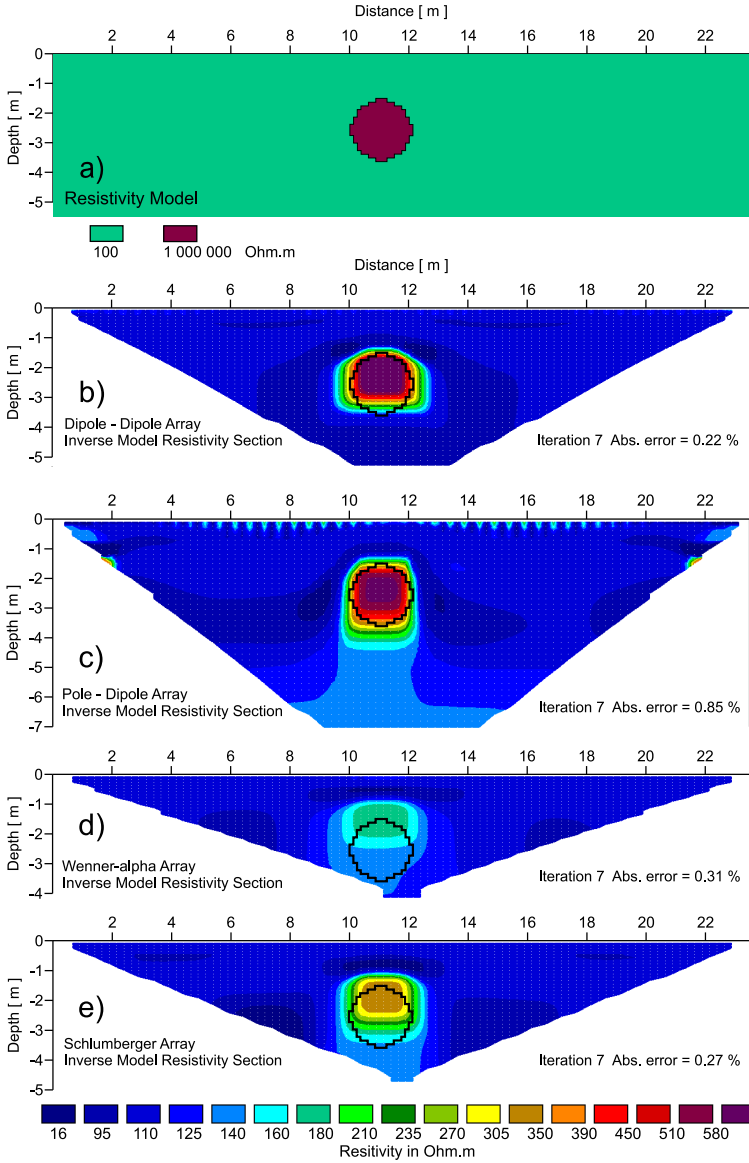


Fig. 2. Inverse model resistivity sections from synthetic data set for  $\rho_2/\rho_1 = 1.0$ : a) geometry of the synthetic model, b) dipole-dipole array, c) pole-dipole array, d) Wenner-alpha array, e) Schlumberger array. The real position of the cavity is plotted on each inverse section.

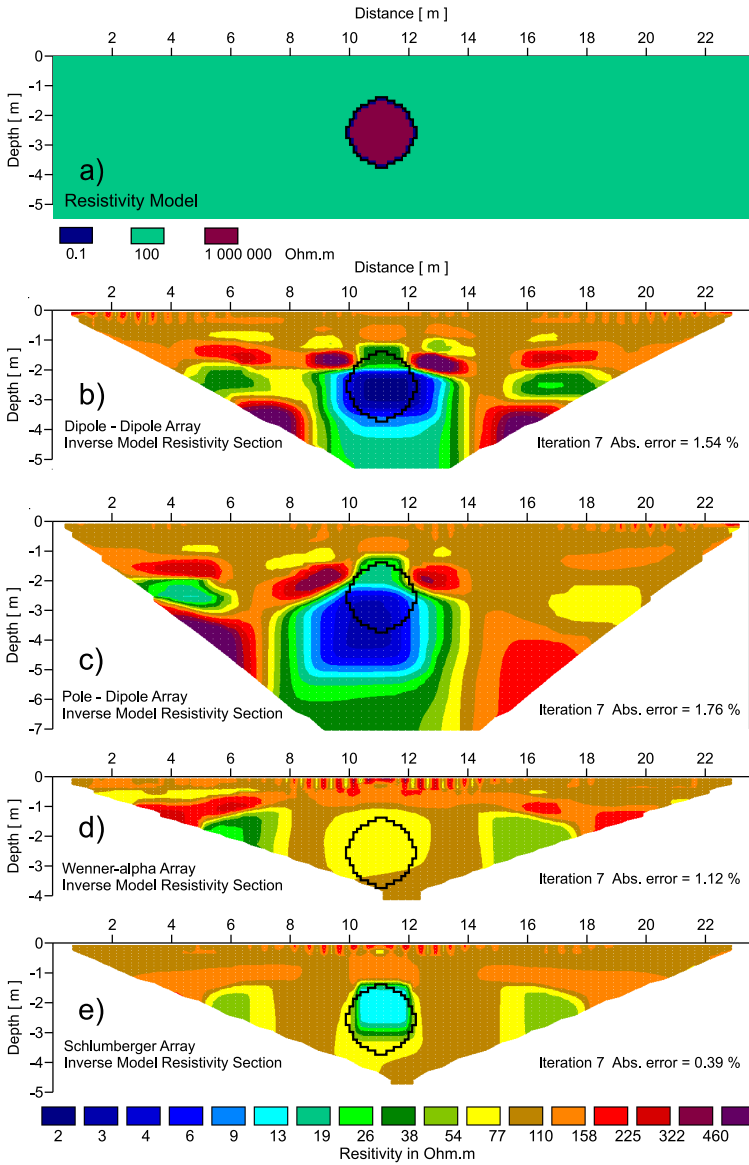


Fig. 3. Inverse model resistivity sections from synthetic data set for  $\rho_2/\rho_1 = 0.001$ : a) geometry of the synthetic model, b) dipole-dipole array, c) pole-dipole array, d) Wenner-alpha array, e) Schlumberger array.

sation method tends to produce models that are piecewise constant (*Ellis and Oldenburg, 1994*). The data sets used in this work have been inverted using the **I<sub>1</sub> norm** inversion method with diagonal filter. For the **I<sub>1</sub> norm** inversion method it is better to use a model where the number of model cells exceeds the number of data points (*Loke et al., 2003*) what eliminates the effect of the block. The **I<sub>1</sub> norm** inversion with wide model blocks gave images that were too “blocky” (*Putiška et al., 2012*). Hence, only the results of the **I<sub>1</sub> norm** inversion with diagonal filter are included in the following discussion. All calculations have been done using the RES2DMOD (*Loke, 2002*) software. All models have been saved as the data of the apparent resistivity without topographic information and without any noise.

### 3. Test results

RES2DINV (*Loke, 2001*) software has been used for calculating the inverse problem from calculated apparent resistivity value of the model. The resulting pseudosections are shown on Figs. 2, 3. It is apparent that different arrays produce significantly different profiles (images).

Figure 2 shows the model without conductivity layer around the cavity. The ratio between air-filled cavity and the surrounding is  $\rho_2/\rho_1$  is 1.0 ( $\rho_2 = \rho_1 = 100 \Omega \text{ m}$ ). The profile from the dipole–dipole (DD) and the combined pole-dipole (CPD) arrays (Fig. 2b, 2c) show very good results. From the inversion results it is clearly seen that the resistivity contrast between the anomalous part and background resistivity is about 600:100  $\Omega \text{ m}$  and the geometry and cavity position correlate well with the model settings. The inversion results lead us to conclude that the DD and CPD electrode arrays are most suitable for the air filled cavity detection. The Wenner-alpha (WA) (Fig. 2d) is the least sensitive electrode array to isometric body among the selected arrays. The resistivity contrast in the inverse image between the cavity and surrounding rock environment is very low (about 200:100  $\Omega \text{ m}$ ). Also the geometry and position of the cavity in the inverse image is significantly moved upwards, what leads us to conclude that the WA electrode array is not able to image reliably the geometry of such a cavity (Fig. 2d). On the inverse section from the SCH array (Fig. 2e) the resistivity contrast between the anomaly and surrounding rock environment is approximately

360:100  $\Omega$  m, better than WA, but still poor result comparing to the DD and CPD arrays. Also the geometry is deformed in very similar way as for WA, what leads to a conclusion that the SCH array is able to locate the cavity but with unreliable geometry.

Figure 3 shows the model with very conductive layer around the air-filled cavity. The ratio between conductive layer and the surrounding is  $\rho_2/\rho_1$  is 0.001 ( $\rho_2 = 0.1 \Omega$  m;  $\rho_1 = 100 \Omega$  m). For all involved electrode arrays (DD, CPD, WA, SCH), the effect of a conductive layer around the air filled cavity (with theoretical infinite resistivity) is very significant as the conductive layer deforms the equipotential lines and the current flows around the cavity in this layer. For the CPD and DD arrays (Fig. 3b, 3c) the mentioned effect resulted in a conductive anomaly in the inverse section, where the ratio between the anomalous part and inverse resistivity of the homogeneous surrounding is about 3:100  $\Omega$  m. The geometry and position of the anomaly show poor correlation with real settings, which is caused by the deformation of the equipotential lines and increased current density in the vicinity of the cavity itself. Furthermore the inverse image of the homogeneous surrounding is disturbed by a number of local resistivity anomalies. The resulting inverse image of WA array (Fig. 3d) yields the ratio between anomalous part and surrounding only about 77:110  $\Omega$  m, what practically means that it is not possible to reliably interpret the cavity from the inverse section. For the SCH array we got similar inverse section as for the WA, however the resistivity ratio between the anomalous resistivity and the homogeneous parts gain better resolution of 13:110  $\Omega$  m.

Based on the test results (Figs. 2, 3), the DD array has been selected as the most accurate and reliable electrode setting for cavity detection surveys and used this array for a series of tests with changing the resistivity  $\rho_2$  0.1, 1.0, 5.0, 7.5, 10.0, 15.0, 20.0, 30.0, 60.0, 90.0 and 100.0  $\Omega$  m, what corresponds with the resistivity ratio  $\rho_2/\rho_1 = 0.001, 0.01, 0.05, 0.075, 0.1, 0.15, 0.2, 0.3, 0.6, 0.9$  and 1.0, respectively. Values of inverse resistivity functions above the centre of the cavity are shown in Fig. 4. Curves for the resistivity contrast  $\rho_2/\rho_1 < 0.1$  show that the cavity appears in the inverse image as a conductive body and the curves  $\rho_2/\rho_1 > 0.1$  refer to a nonconductive body. For the case that resistivity contrast ratio  $\rho_2/\rho_1 \approx 0.1$ , the anomalous response of the cavity is barely readable from the inverse section. The 2D sections for this case are shown in Fig. 5.

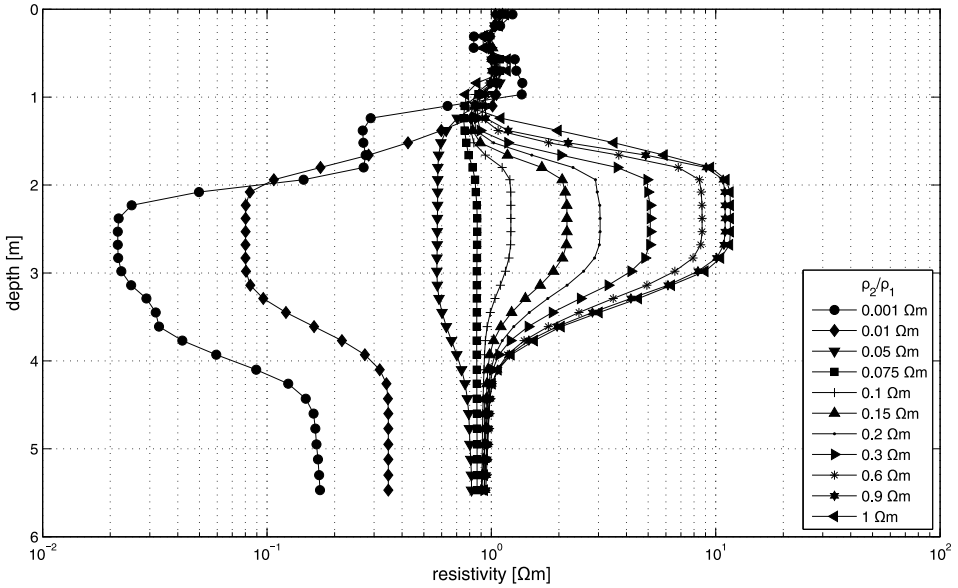


Fig. 4. Comparison of the 1D inverse resistivity values for the DD array on the  $x = 11$  m (centre of the cavity), for different resistivity contrast between the conductive layer  $\rho_2$  and homogeneous background  $\rho_1$ .

### 4. Conclusions

The results presented in the previous section indicate that the anomalous image of the cavity in the inverse section is highly depending on the ratio  $\rho_2/\rho_1$  (resistivity of the thin layer around the cavity/resistivity of the background). In this case, the thin layer around the cavity is more conductive than the surrounding material, the conductivity of the layer causes a deformation of the equipotential lines and increases the current density, so the current flows around the high resistive cavity, what leads to an effect that the air-filled cavity with very high resistivity appears on the inverse section as conductive; also an interesting inverse effect occurs when the homogeneous background is not reconstructed correctly and a number of false resistivity anomalies is created in the inverse image (Figs. 3 and 5). By increasing the resistivity of the layer close to the ratio  $\rho_2/\rho_1 = 0.1$ , the anomalous feature

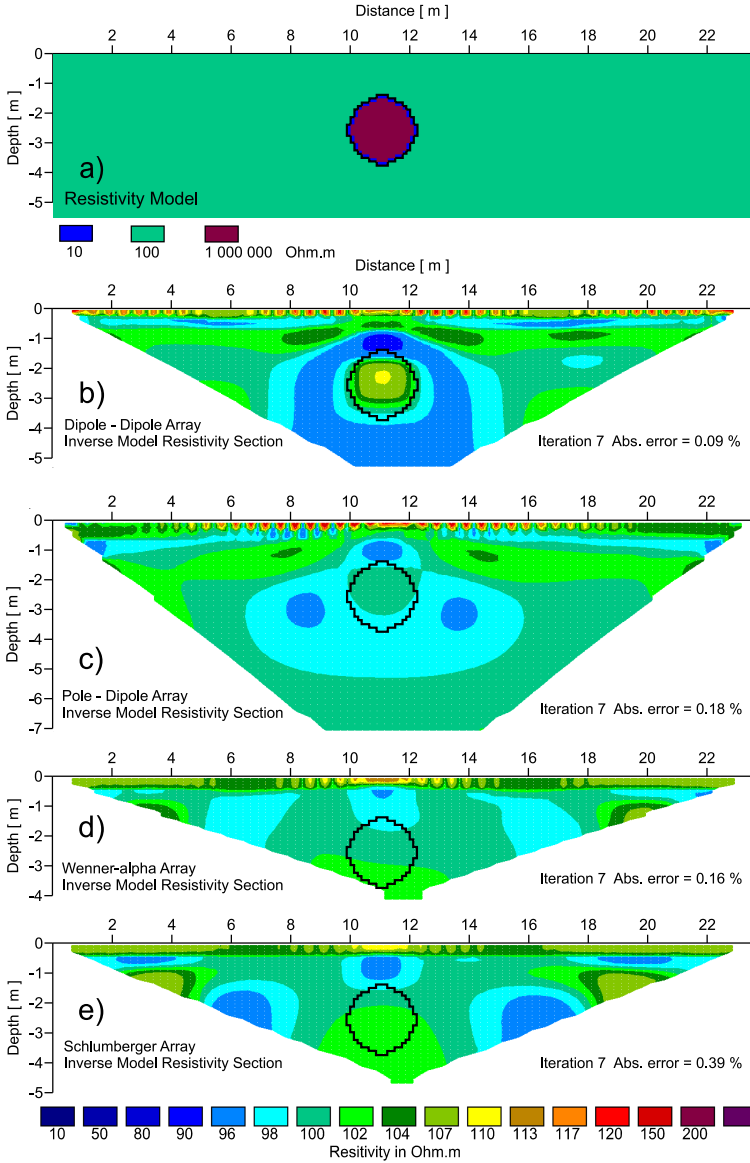


Fig. 5. Inverse model resistivity sections from synthetic data set for  $\rho_2/\rho_1 = 0.1$ : a) geometry of the synthetic model, b) dipole-dipole array, c) pole-dipole array, d) Wenner-alpha array, e) Schlumberger array.

of the cavity in the inverse section is barely visible, and the utilization of the resistivity methods is very limited for such a case. By further increasing the ratio  $\rho_2/\rho_1$  above the value 0.1, the cavity becomes to be a resistive anomaly in the inverse section and the potential of detection by means of resistivity methods is very good. From the modelling outputs (Figs. 2 and 3) it is possible to state that the CPD a DD arrays are much more suitable for isometric body detection (cavity), with detailed and reliable geometry estimation, than other involved electrode arrays (WA, SCH).

**Acknowledgments.** The authors are grateful to the Slovak Grant Agency VEGA (grant nos. 1/0747/11, 1/0095/12, 2/0067/12), UK/530/2012 and the Slovak Research and Development Agency APVV (grant nos. APVV-0194-10) for the support of their research.

## References

- Cardarelli E., Di Filippo G., Tuccinardi E., 2006a: Electrical resistivity tomography to detect buried cavities in Rome: a case study. *Near Surface Geophysics*, **4**, 387–392.
- Cardarelli E., Fischanger F., 2006b: 2D data modelling by electrical resistivity tomography for complex subsurface geology. *Geophysical Prospecting*, **54**, 121–134.
- Chalikakis K., Plagnes V., Guerin R., Valois R., Bosch F. P., 2011: Contribution of geophysical methods to karst-system exploration: an overview. *Hydrogeology Journal*, **19**, 1169–1180.
- Cook K. L., Van Nostrand R. G., 1954: Interpretation of resistivity data over filled sinks. *Geophysical Prospecting*, **21**, 716–723.
- Dutta N., Bose R., Saikia B., 1970: Detection of solution channels in limestone by electrical resistivity method. *Geophysical Prospecting*, **18**, 405–414.
- Ellis R. G., Oldenburg D. W., 1994: Applied geophysical inversion. *Geophysical Journal International*, **116**, 5–11.
- Greenfield R. J., 1979: Review of geophysical approaches to the detection of karst. *Bull. Assoc. Eng. Geol.*, **16**, 393–408.
- Hutchinson D. J., Phillips C., Cascante G., 2002: Risk considerations for crown pillar stability assessment for mine closure planning. *J. Geotech. Geol. Eng.*, **20**, 41–64.
- Loke M. H., 1997: Rapid 2D resistivity inversion using the least-squares method. RES2-DINV Program manual, Penang, Malaysia.
- Loke M. H., 2001: Tutorial: 2-D and 3-D electrical imaging surveys. Geotomo Software, Malaysia.
- Loke M. H., 2002: Rapid 2D resistivity forward modeling using the finite-difference and finite-element methods. Geotomo Software, Malaysia.

- Loke M. H., Acworth I., Dahlin T., 2003: A comparison of smooth and blocky inversion methods in 2D electrical imaging surveys. *Exploration Geophysics*, **34**, 182–187.
- Militzer H., Rösler R., Lösch W., 1979: Theoretical and experimental investigations for cavity research with geoelectrical resistivity methods. *Geophysical Prospecting*, **27**, 640–652.
- Olayinka A. I., Yaramanci U., 2000: Use of block inversion in the 2-D interpretation of apparent resistivity data and its comparison with smooth inversion. *Journal of Applied Geophysics*, **45**, 63–81.
- Putiška R., Dostál I., Kušnirák D., 2012: Determination of dipping contacts using electrical resistivity tomography. *Contrib. Geophys. Geod.*, **42**, 2, 161–180.
- Smith D. L., 1986: Application of the pole–dipole resistivity technique to the detection of solution cavities beneath highways. *Geophysics*, **51**, 833–837.
- Thomas B., Roth M. J. S., 1999: Evaluation of site characterization methods for inkholes in Pennsylvania and New Jersey. *Eng. Geol.*, **52**, 147–152.
- Van Schoor M., 2002: Detection of sinkholes using 2D electrical resistivity imaging. *Journal of Applied Geophysics*, **50**, 393–399.
- Vincenz A., 1968: Resistivity investigations of limestone aquifers in Jamaica. *Geophysics*, **33**, 980–994.
- Zhou W., Beck B. F., Adams A. L., 2002: Effective electrode array in mapping karst hazards in electrical resistivity tomography. *Environ. Geol.*, **42**, 922–928.